151. Chemical Selectivities Disguised by Mass Diffusion. VII. A Simple Model of pH-Dependence of Product Distribution in Mixing-Disguised Azo Coupling Reactions[1][2])

8th Communication on the Selectivity of Chemical Processes[1])

by **Hasan Belevi, John R. Bourne** and **Paul Rys**

Technisch-Chemisches Laboratorium, Eidgenössische Technische Hochschule, CH-8092 Zürich

Dedicated to the memory of Prof. *Norbert Ibl*

(13.V.81)

Summary

In the present work a mixing-reaction model is developed to describe the influence of the space- and time-dependent concentration of the leaving group on the pre-equilibria of the reactants and thus on the product distribution of mixing-disguised reactions. The modelling is carried out using a typical example of such reactions, namely azo coupling, where the leaving group is a proton. For this reaction, the existence of characteristic sets of parameters is established, for which the product distribution does not depend on the initial pH-value. These sets of parameters define the isoselectivity points.

1. Introduction. – When two reagent solutions are brought into contact and react rapidly before achieving perfect mixing on the molecular scale, the intrinsic kinetics of the chemical reaction can be disguised by mixing processes. In previous parts of this series a mixing-reaction model MIRE has been developed, which allows a description of the coupling of the diffusive mixing process with the bond-making and bond-breaking events of the chemical reaction [3–5]. In those mixing-disguised reactions where the products influence the local concentrations of the reactants in the reaction zone, the diffusion process of the products as well as of the reactants determines the selectivity. This phenomenon has been demonstrated in fast bromination [6] and azo coupling [7] reactions, however, up to now only in a qualitative way. For example, in the azo coupling of aromatic compounds the proton which is released during the electrophilic substitution step causes a local pH-gradient. The local concentrations of reactants are then changed as a consequence of shifts in the acid-base equilibria of the diazo and the coupling components. If the azo coupling reactions are faster than the diffusion of the released protons out of the reaction zone, the local pH-gradients will disguise the selectivity.

[1]) Part VI and 7th Communication *cf.* [1].

[2]) Results taken from the Ph. D. thesis of *H. Belevi* [2].

0018-019X/81/5/1599-19$01.00/0

In the present paper, the MIRE-model will be extended (MIRE-PH) to calculate the influence of the space- and time-dependent concentration of the products on the preequilibria of the reactants and thus on the products of mixing-disguised reactions. A competitive, consecutive azo coupling reaction is chosen to illustrate such phenomena.

2. The Concept of the Mixing-Reaction Model 'MIRE-PH'. – In the previous parts I [3] and III [4] the MIRE-model has been described in detail. Version II of the MIRE-model (MIRE-2) can briefly be outlined as follows: If a solution of a species B is added to a solution of a species A, eddies of solution B in solution A are created. The dispersion of the eddies throughout the whole liquid is assumed to be faster than the molecular diffusion within them. Consequently, the concentration gradients around the eddies can be neglected.

As a first approximation the eddies can be assumed spherical with a constant mean radius $\bar{R}$[3]). $\bar{R}$ can be roughly estimated by the theory of turbulence as equal to the *Kolmogoroff* velocity microscale λ_K [8], whereby $\lambda_K = 2 \cdot \bar{R}$.

The species B is considered to be immobile in the eddy and all other species are considered to be mobile. This simplification reduces substantially the time for computer calculations without falsifying the general qualitative conclusions about mixing effects in fast reactions.

For the description of the selectivity of mixing-disguised consecutive azo coupling reactions, a similar but more detailed mixing reaction model has to be developed. It has to take into account that, for an insufficient buffer capacity in the reaction zone, the proton released in the substitution step may influence the concentration of the reactants.

For the modelling the following reactions and pre-equilibria have to be considered *(Scheme)*[4]):

Scheme

Azo Coupling Reactions:

$$AO^{\ominus} + ArN_2^{\oplus} \xrightarrow{k_{1,m}} RO^{\ominus} + H^{\oplus} \tag{1}$$

$$RO^{\ominus} + ArN_2^{\oplus} \xrightarrow{k_{2,m}} SO^{\ominus} + H^{\oplus} \tag{2}$$

Acid Base Equilibria:

$$AOH \underset{k_{-A}}{\overset{k_A}{\rightleftharpoons}} AO^{\ominus} + H^{\oplus} \tag{3}$$

$$ROH \underset{k_{-R}}{\overset{k_R}{\rightleftharpoons}} RO^{\ominus} + H^{\oplus} \tag{4}$$

$$SOH \underset{k_{-S}}{\overset{k_S}{\rightleftharpoons}} SO^{\ominus} + H^{\oplus} \tag{5}$$

---

[3]) Calculations have shown that linear, cyclindrical or time dependent geometries give other results. Because of the higher surface-to-volume ratio, every other geometry of the eddy having the same volume shows a lower disguising effect of diffusion of the selectivity. However, the general behaviour is the same. A comprehensive discussion is in preparation.

[4]) A detailed description of this reaction system has been given elsewhere [2] [7]. For definition of symbols, see Appendix at the end.

$$ArN_2^{\oplus} + H_2O \underset{k_{-B,1}}{\overset{k_{B,1}}{\rightleftharpoons}} ArN_2OH + H^{\oplus} \underset{k_{-B,2}}{\overset{k_{B,2}}{\rightleftharpoons}} ArN_2O^{\ominus} + 2\,H^{\oplus} \tag{6}$$

$$P^a \underset{k_{-P}}{\overset{k_P}{\rightleftharpoons}} P^b + H^{\oplus} \tag{7}$$

$$H_2O \underset{k_{-H_2O}}{\overset{k_{H_2O}}{\rightleftharpoons}} H^{\oplus} + OH^{\ominus} \tag{8}$$

If we assume an isothermal system, incompressible liquids, spherical eddies and dilute solutions, a material balance for species i leads to the diffusion-reaction equation 9.

$$\frac{\partial [i]}{\partial t} = D_i \left(\frac{\partial^2 [i]}{\partial r^2} + \frac{2}{r} \frac{\partial [i]}{\partial r} \right) + r_i \tag{9}$$

For simplicity one can make the following additional restrictions [2] [9]:

- The pH-value is low enough that the concentration of the free diazonium ion will equal the total concentration of the diazo component ($[ArN_2^{\oplus}] = [B]$).
- The diffusivity D is the same for all mobile species ($D_i = D$). For the immobile species B the diffusivity is zero ($D_B = 0$).
- The reaction conditions are chosen in such a way that the substitution step shows no general base catalysis. Otherwise, a more detailed modelling is needed which leads to base-dependent rate constants.

Hence, for the azo coupling reaction system which is given in the *Scheme*, the following partial differential equations result:

$$\frac{\partial [AO^{\ominus}]}{\partial t} = D \left(\frac{\partial^2 [AO^{\ominus}]}{\partial r^2} + \frac{2}{r} \frac{\partial [AO^{\ominus}]}{\partial r} \right) - k_{l,m} [AO^{\ominus}][B] + k_A [AOH][OH^{\ominus}] - k_{-A} [AO^{\ominus}] \tag{10}$$

$$\frac{\partial [AOH]}{\partial t} = D \left(\frac{\partial^2 [AOH]}{\partial r^2} + \frac{2}{r} \frac{\partial [AOH]}{\partial r} \right) + k_{-A} [AO^{\ominus}] - k_A [AOH][OH^{\ominus}] \tag{11}$$

$$\frac{\partial [RO^{\ominus}]}{\partial t} = D \left(\frac{\partial^2 [RO^{\ominus}]}{\partial r^2} + \frac{2}{r} \frac{\partial [RO^{\ominus}]}{\partial r} \right) + k_{l,m} [AO^{\ominus}][B] - k_{2,m} [RO^{\ominus}][B] + k_R [ROH][OH^{\ominus}] - k_{-R} [RO^{\ominus}] \tag{12}$$

$$\frac{\partial [ROH]}{\partial t} = D \left(\frac{\partial^2 [ROH]}{\partial r^2} + \frac{2}{r} \frac{\partial [ROH]}{\partial r} \right) + k_{-R} [RO^{\ominus}] - k_R [ROH][OH^{\ominus}] \tag{13}$$

$$\frac{\partial [SO^{\ominus}]}{\partial t} = D \left(\frac{\partial^2 [SO^{\ominus}]}{\partial r^2} + \frac{2}{r} \frac{\partial [SO^{\ominus}]}{\partial r} \right) + k_{2,m} [RO^{\ominus}][B] + k_S [SOH][OH^{\ominus}] - k_{-S} [SO^{\ominus}] \tag{14}$$

$$\frac{\partial [SOH]}{\partial t} = D \left(\frac{\partial^2 [SOH]}{\partial r^2} + \frac{2}{r} \frac{\partial [SOH]}{\partial r} \right) + k_{-S} [SO^{\ominus}] - k_S [SOH][OH^{\ominus}] \tag{15}$$

$$\frac{\partial [P^s]}{\partial t} = D\left(\frac{\partial^2 [P^s]}{\partial r^2} + \frac{2}{r}\frac{\partial [P^s]}{\partial r}\right) - k_P [P^s][OH^\ominus] + k_{-P}[P^b] \tag{16}$$

$$\frac{\partial [P^b]}{\partial t} = D\left(\frac{\partial^2 [P^b]}{\partial r^2} + \frac{2}{r}\frac{\partial [P^b]}{\partial r}\right) + k_P [P^s][OH^\ominus] - k_{-P}[P^b] \tag{17}$$

$$\begin{aligned}\frac{\partial [OH^\ominus]}{\partial t} = {} & D\left(\frac{\partial^2 [OH^\ominus]}{\partial r^2} + \frac{2}{r}\frac{\partial [OH^\ominus]}{\partial r}\right) + k_{-A}[AO^\ominus] - k_A [AOH][OH^\ominus] \\ & + k_{-R}[RO^\ominus] - k_R [ROH][OH^\ominus] + k_{-S}[SO^\ominus] - k_S [SOH][OH^\ominus] \\ & + k_{-P}[P^b] - k_P [P^s][OH^\ominus] + k_{H_2O}[H_2O] - k_{-H_2O}[H^\oplus][OH^\ominus]\end{aligned} \tag{18}$$

$$\begin{aligned}\frac{\partial [H^\oplus]}{\partial t} = {} & D\left(\frac{\partial^2 [H^\oplus]}{\partial r^2} + \frac{2}{r}\frac{\partial [H^\oplus]}{\partial r}\right) + k_{1,m}[AO^\ominus][B] + k_{2,m}[RO^\ominus][B] \\ & + k_{H_2O}[H_2O] - k_{-H_2O}[H^\oplus][OH^\ominus]\end{aligned} \tag{19}[5]$$

$$\frac{\partial [B]}{\partial t} = -k_{1,m}[AO^\ominus][B] - k_{2,m}[RO^\ominus][B] \tag{20}$$

In order to reduce the time for the computer calculations the following reduction of the equations 10–20 is made: When the parameter $[H^\oplus]_t$ is introduced the equations 11, 13, 15, 16, 18 and 19 can be combined with each other, *i.e.*

$$[H^\oplus]_t = [H^\oplus] - [OH^\ominus] + [P^s] + [AOH] + [ROH] + [SOH] \tag{21}$$

Hence it follows that

$$\frac{\partial [H^\oplus]_t}{\partial t} = D\left(\frac{\partial^2 [H^\oplus]_t}{\partial r^2} + \frac{2}{r}\frac{\partial [H^\oplus]_t}{\partial r}\right) + k_{1,m}[AO^\ominus][B] + k_{2,m}[RO^\ominus][B] \tag{22}$$

In like manner the equations 10 with 11, 12 with 13, 14 with 15 and 16 with 17 can be combined. Introducing total concentration for A, R, S and P one obtains the differential equations 23–26.

$$\frac{\partial [A]}{\partial t} = D\left(\frac{\partial^2 [A]}{\partial r^2} + \frac{2}{r}\frac{\partial [A]}{\partial r}\right) - k_{1,m}[AO^\ominus][B] \tag{23}$$

$$\frac{\partial [R]}{\partial t} = D\left(\frac{\partial^2 [R]}{\partial r^2} + \frac{2}{r}\frac{\partial [R]}{\partial r}\right) + k_{1,m}[AO^\ominus][B] - k_{2,m}[RO^\ominus][B] \tag{24}$$

$$\frac{\partial [S]}{\partial t} = D\left(\frac{\partial^2 [S]}{\partial r^2} + \frac{2}{r}\frac{\partial [S]}{\partial r}\right) + k_{2,m}[RO^\ominus][B] \tag{25}$$

$$\frac{\partial [P]}{\partial t} = D\left(\frac{\partial^2 [P]}{\partial r^2} + \frac{2}{r}\frac{\partial [P]}{\partial r}\right) \tag{26}$$

[5] The symbol $H^\oplus$ stands for hydronium ion and higher hydrated proton.

The relations 27–30 define the total concentrations of A, R, S and P.

$$[A]=[AOH]+[AO^{\ominus}] \tag{27}$$

$$[R]=[ROH]+[RO^{\ominus}] \tag{28}$$

$$[S]=[SOH]+[SO^{\ominus}] \tag{29}$$

$$[P]=[P^{s}]+[P^{b}] \tag{30}$$

The neutralisation reactions are generally much faster than the azo coupling reactions [10]. Thus the neutral forms of the species A, R and S and the acidic form of P can be described by their total concentrations, their acidity constants and the proton concentration.

$$[AOH]=\frac{[A][H^{\oplus}]}{K_A+[H^{\oplus}]} \tag{31}$$

$$[ROH]=\frac{[R][H^{\oplus}]}{K_R+[H^{\oplus}]} \tag{32}$$

$$[SOH]=\frac{[S][H^{\oplus}]}{K_S+[H^{\oplus}]} \tag{33}$$

$$[P^{s}]=\frac{[P][H^{\oplus}]}{K_P+[H^{\oplus}]} \tag{34}$$

The concentration of the hydroxyl ion can be calculated with the help of the ionisation constant K_W.

$$[OH^{\ominus}]=\frac{K_W}{[H^{\oplus}]} \tag{35}$$

Thus, the relations 21–35 enable one to reduce the diffusion-reaction equations 10–20 to the equations 36–42.

$$\frac{\partial[A]}{\partial t}=D\left(\frac{\partial^2[A]}{\partial r^2}+\frac{2}{r}\frac{\partial[A]}{\partial r}\right)-\frac{k_{1,m}K_A}{K_A+[H^{\oplus}]}[A][B] \tag{36}$$

$$\frac{\partial[R]}{\partial t}=D\left(\frac{\partial^2[R]}{\partial r^2}+\frac{2}{r}\frac{\partial[R]}{\partial r}\right)+\frac{k_{1,m}K_A}{K_A+[H^{\oplus}]}[A][B]-\frac{k_{2,m}K_R}{K_R+[H^{\oplus}]}[R][B] \tag{37}$$

$$\frac{\partial[S]}{\partial t}=D\left(\frac{\partial^2[S]}{\partial r^2}+\frac{2}{r}\frac{\partial[S]}{\partial r}\right)+\frac{k_{2,m}K_R}{K_R+[H^{\oplus}]}[R][B] \tag{38}$$

$$\frac{\partial [H^{\oplus}]_t}{\partial t} = D\left(\frac{\partial^2 [H^{\oplus}]_t}{\partial r^2} + \frac{2}{r}\frac{\partial [H^{\oplus}]_t}{\partial r}\right) + \frac{k_{1,m} K_A}{K_A + [H^{\oplus}]}[A][B] + \frac{k_{2,m} K_R}{K_R + [H^{\oplus}]}[R][B] \quad (39)$$

$$\frac{\partial [P]}{\partial t} = D\left(\frac{\partial^2 [P]}{\partial r^2} + \frac{2}{r}\frac{\partial [P]}{\partial r}\right) \quad (40)$$

$$\frac{\partial [B]}{\partial t} = -\frac{k_{1,m} K_A}{K_A + [H^{\oplus}]}[A][B] - \frac{k_{2,m} K_R}{K_R + [H^{\oplus}]}[R][B] \quad (41)$$

$$[H^{\oplus}]_t = [H^{\oplus}] - \frac{K_W}{[H^{\oplus}]} + [H^{\oplus}]\left(\frac{[A]}{K_A + [H^{\oplus}]} + \frac{[R]}{K_R + [H^{\oplus}]} + \frac{[S]}{K_S + [H^{\oplus}]} + \frac{[P]}{K_P + [H^{\oplus}]}\right) \quad (42)$$

The equations 36–42 with the corresponding initial and boundary conditions describe the diffusion-reaction process completely.

The initial conditions result from the state of the mixture immediately after the dispersion of the fresh B-rich solution in A-rich solution ($t = 0$):

$$r < \bar{R}: \quad [A] = 0; \quad [R] = 0; \quad [S] = 0$$
$$[H^{\oplus}] = [H^{\oplus}]_0; \quad [B] = [B]_0; \quad [P] = [P]_0 \quad (43)$$

$$r = \bar{R}: \quad [A] = [A]_0; \quad [R] = 0; \quad [S] = 0$$
$$[H^{\oplus}] = [H^{\oplus}]_0; \quad [B] = [B]_0; \quad [P] = [P]_0 \quad (44)$$

One boundary condition for each partial differential equation results from the fact that no concentration gradient arises at the center of the eddy owing to the symmetry of the sphere.

$$r = 0: \frac{\partial [A]}{\partial r} = \frac{\partial [R]}{\partial r} = \frac{\partial [S]}{\partial r} = \frac{\partial [H^{\oplus}]_t}{\partial r} = \frac{\partial [P]}{\partial r} = 0 \quad (45)$$

A further boundary condition results from the requirement that the change in the amount of dissolved species i in the surrounding solution has to correspond to the flux of species i which diffuses through the surface of the eddy [2] [4].

$$r = \bar{R}: \frac{\partial [A]}{\partial t} = -3\frac{V_B}{V_A}\frac{D}{\bar{R}}\frac{\partial [A]}{\partial r} \quad (46)$$

$$\frac{\partial [R]}{\partial t} = -3\frac{V_B}{V_A}\frac{D}{\bar{R}}\frac{\partial [R]}{\partial r} \quad (47)$$

$$\frac{\partial [S]}{\partial t} = -3\frac{V_B}{V_A}\frac{D}{\bar{R}}\frac{\partial [S]}{\partial r} \quad (48)$$

$$\frac{\partial [H^{\oplus}]_t}{\partial t} = -3 \frac{V_B}{V_A} \frac{D}{\bar{R}} \frac{\partial [H^{\oplus}]_t}{\partial r} \tag{49}$$

$$\frac{\partial [P]}{\partial t} = -3 \frac{V_B}{V_A} \frac{D}{\bar{R}} \frac{\partial [P]}{\partial r} \tag{50}$$

The equations 36–50 can be normalized by introducing the following dimensionless parameters:

$$T = \frac{D}{\bar{R}^2} t; \qquad X = \frac{r}{\bar{R}}; \qquad \alpha = \frac{V_A}{V_B}; \qquad E = \frac{[A]_0}{[B]_0}$$

$$A_A = \frac{[A]}{[A]_0}; \qquad B_B = \frac{[B]}{[B]_0}; \qquad \Omega_A = \frac{[R]}{[A]_0}; \qquad \Psi_A = \frac{[S]}{[A]_0}$$

$$H_A = \frac{[H^{\oplus}]}{[A]_0}; \qquad \Theta_A = \frac{[H^{\oplus}]_t}{[A]_0}; \qquad \Pi_A = \frac{[P]}{[A]_0}; \qquad K_W = \frac{K_W}{[A]_0^2}$$

$$K_A = \frac{K_A}{[A]_0}; \qquad K_R = \frac{K_R}{[A]_0}; \qquad K_S = \frac{K_S}{[A]_0}; \qquad K_P = \frac{K_P}{[A]_0}$$

$$\varphi^2_{B,1,m} = \frac{k_{1,m} \bar{R}^2 [B]_0}{D}; \qquad \varphi^2_{B,2,m} = \frac{k_{2,m} \bar{R}^2 [B]_0}{D}$$

This generalisation leads to the equations 51–57 and to the inital and the boundary conditions 58–65 describing the diffusion-reaction process given in the *Scheme:*

$$\frac{\partial A_A}{\partial T} = \frac{\partial^2 A_A}{\partial X^2} + \frac{2}{X} \frac{\partial A_A}{\partial X} - \varphi^2_{B,1,m} \frac{K_A}{K_A + H_A} A_A B_B \tag{51}$$

$$\frac{\partial \Omega_A}{\partial T} = \frac{\partial^2 \Omega_A}{\partial X^2} + \frac{2}{X} \frac{\partial \Omega_A}{\partial X} + \varphi^2_{B,1,m} \frac{K_A}{K_A + H_A} A_A B_B - \varphi^2_{B,2,m} \frac{K_R}{K_R + H_A} \Omega_A B_B \tag{52}$$

$$\frac{\partial \Psi_A}{\partial T} = \frac{\partial^2 \Psi_A}{\partial X^2} + \frac{2}{X} \frac{\partial \Psi_A}{\partial X} + \varphi^2_{B,2,m} \frac{K_R}{K_R + H_A} \Omega_A B_B \tag{53}$$

$$\frac{\partial \Theta_A}{\partial T} = \frac{\partial^2 \Theta_A}{\partial X^2} + \frac{2}{X} \frac{\partial \Theta_A}{\partial X} + \varphi^2_{B,1,m} \frac{K_A}{K_A + H_A} A_A B_B + \varphi^2_{B,2,m} \frac{K_R}{K_R + H_A} \Omega_A B_B \tag{54}$$

$$\frac{\partial B_B}{\partial T} = -E \varphi^2_{B,1,m} \frac{K_A}{K_A + H_A} A_A B_B - E \varphi^2_{B,2,m} \frac{K_R}{K_R + H_A} \Omega_A B_B \tag{55}$$

$$\frac{\partial \Pi_A}{\partial T} = \frac{\partial^2 \Pi_A}{\partial X^2} + \frac{2}{X}\frac{\partial \Pi_A}{\partial X} \tag{56}$$

$$\Theta_A = H_A - \frac{K_W}{H_A} + H_A\left(\frac{A_A}{K_A + H_A} + \frac{\Omega_A}{K_R + H_A} + \frac{\Psi_A}{K_S + H_A} + \frac{\Pi_A}{K_P + H_A}\right) \tag{57}$$

Initial conditions: $T = 0$

$$X < 1: \quad A_A = 0; \quad B_B = 1; \quad \Omega_A = 0; \quad \Psi_A = 0; \quad H_A = H_{A,0}; \quad \Pi_A = \Pi_{A,0} \tag{58}$$

$$X = 1: \quad A_A = 1; \quad B_B = 1; \quad \Omega_A = 0; \quad \Psi_A = 0; \quad H_A = H_{A,0}; \quad \Pi_A = \Pi_{A,0} \tag{59}$$

Boundary conditions: $T > 0$

$$X = 0: \frac{\partial A_A}{\partial X} = \frac{\partial \Omega_A}{\partial X} = \frac{\partial \Psi_A}{\partial X} = \frac{\partial \Theta_A}{\partial X} = \frac{\partial \Pi_A}{\partial X} = 0 \tag{60}$$

$$X = 1: \frac{\partial A_A}{\partial T} = -\frac{3}{\alpha}\frac{\partial A_A}{\partial X} \tag{61}$$

$$\frac{\partial \Omega_A}{\partial T} = -\frac{3}{\alpha}\frac{\partial \Omega_A}{\partial X} \tag{62}$$

$$\frac{\partial \Psi_A}{\partial T} = -\frac{3}{\alpha}\frac{\partial \Psi_A}{\partial X} \tag{63}$$

$$\frac{\partial \Theta_A}{\partial T} = -\frac{3}{\alpha}\frac{\partial \Theta_A}{\partial X} \tag{64}$$

$$\frac{\partial \Pi_A}{\partial T} = -\frac{3}{\alpha}\frac{\partial \Pi_A}{\partial X} \tag{65}$$

In the calculations and in the experiments (*cf.* Part VIII [9]) the initial concentrations of the buffer in the eddy as well as in the surrounding solution are chosen to be equal. Consequently, the diffusion equation 56 and the boundary conditions 58, 59 and 65 for the buffer are redundant.

3. Procedure for Numerical Solution. – An analytical solution for the diffusion-reaction equations 51–55 does not exist yet. Therefore, a computer program in FORTRAN was written for the numerical solution. For the solution of the partial differential equations the subroutines of the simulation package FORSIM-V were used, and for the solution of equation 57 the secant method (iteration) was used [2].

The calculations were carried out on a CDC computer.
All the simulations were calculated up to 99.95% conversion of B.

4. Results. – The product distribution X_S is given by the following relation after 100% conversion of B:

$$X_S = \frac{2\Psi_A}{2\Psi_A + \Omega_A} \tag{66}$$

The diffusion-reaction process is determined for given initial and boundary conditions by the parameters E, α, $\varphi^2_{B,1,m}$, $\varphi^2_{B,2,m}$, K_A, K_R, K_S, K_W, K_P, $\Pi_{A,0}$ and $H_{A,0}$. The meaning of the mixing-moduli $\varphi^2_{B,1,m}$ and $\varphi^2_{B,2,m}$ correspond to that of the *Damköhler*-Number [11], the square of *Thiele*-Modulus [12] or the square of the *Hatta*-Number [13]. *Figure 1* shows the influence of the mixing-moduli $\varphi^2_{B,1,m}$ and $\varphi^2_{B,2,m}$ on X_S for a given initial pH-value[6]). With an increase of $\varphi^2_{B,2,m}$, the effect of mixing becomes greater and the product distribution X_S increases. The larger the value of $\varphi^2_{B,1,m}/\varphi^2_{B,2,m}$, the lower is X_S.

A comparison of the calculations at constant pH-values by MIRE-2 *(Fig. 2)*[7]) with the calculated behaviour by MIRE-PH *(Fig. 1)* shows clearly that the release of protons during azo coupling reactions has a great influence on X_S. In *Figure 2* the pH-value remains constant in time as well as locally. The product distribution X_S is sensitive to $\varphi^2_{B,1,m}/\varphi^2_{B,2,m}$ when diffusion has only a slight influence

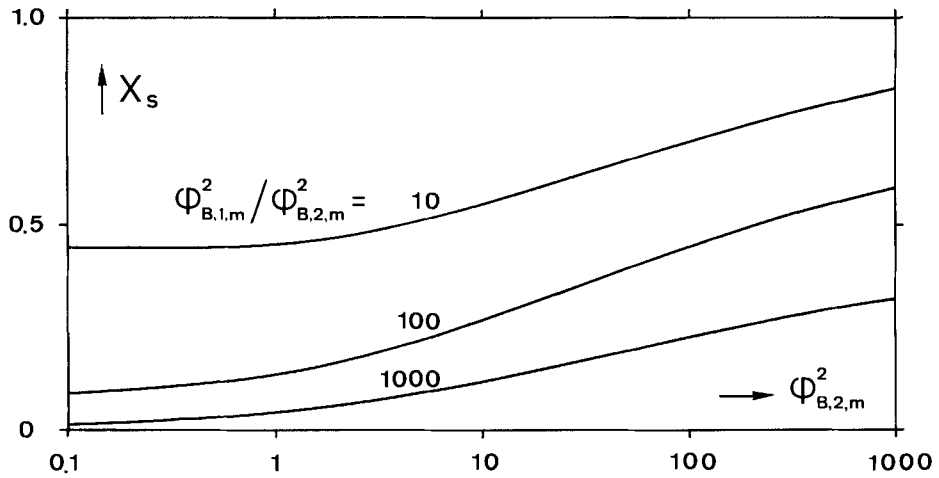

Fig. 1. *Model calculations with MIRE-PH: X_S as a function of $\varphi^2_{B,2,m}$ for different intrinsic selectivities $\varphi^2_{B,1,m}/\varphi^2_{B,2,m}$*
$E = 0{,}1$; $\alpha = 20$; $\Pi_{A,0} = 15$; $K_A = 10^{-7{,}88}$; $K_R = 10^{-6{,}28}$; $K_S = 10^{-6{,}0}$; $K_P = 10^{-8{,}25}$; $K_W = 10^{-12{,}1}$; $H_{A,0} = 10^{-7{,}0}$.

---

[6]) Initial pH-value is $pH = -\log H_{A,0}\,[A]_0$. For a clear interpretation it is convenient to let $[A]_0$ be constant. In this case the different values of $H_{A,0}$ can be considered as a variation of the initial pH-values.

[7]) When $H_{A,0}$ remains constant, the calculations can be carried out with MIRE-2 [2] [7].

Table 1. *Model calculations with MIRE-PH: X_S as a function of $\varphi^2_{B,1,m}$ for different values of $\varphi^2_{B,1,m}/\varphi^2_{B,2,m}$*

$K_A = 10^{-7.88}$; $K_R = 10^{-6.28}$; $K_S = 10^{-6.0}$; $K_P = 10^{-8.25}$; $K_W = 10^{-12.1}$. RC: reaction controlled.

E	α	$\frac{\varphi^2_{B,1,m}}{\varphi^2_{B,2,m}}$	$\varphi^2_{B,2,m}$	$H_{A,0}$	$\Pi_{A,0}$	X_S
0.1	20	10	RC	$10^{-7.0}$	15	0.441
			1			0.455
			10			0.549
			40			0.638
			100			0.697
			400			0.780
			1000			0.826
0.1	20	100	RC	$10^{-7.0}$	15	0.093
			1			0.137
			2			0.166
			10			0.269
			40			0.375
			100			0.443
			400			0.537
			1000			0.588
0.1	20	1000	RC	$10^{-7.0}$	15	0.011
			0.4			0.029
			1			0.044
			4			0.082
			10			0.118
			40			0.182
			100			0.227
			1000			0.320

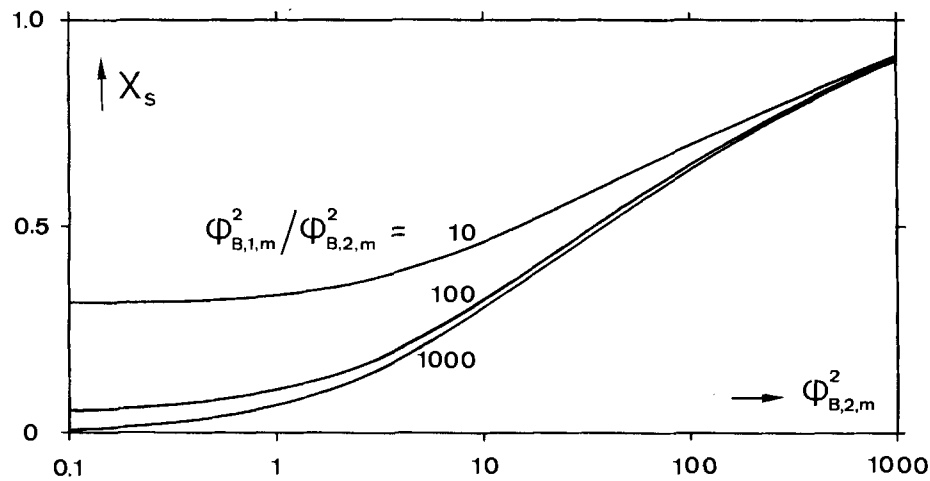

Fig. 2. *Model calculations with MIRE-2: X_S as a function of $\varphi^2_{B,2,m}$ for different intrinsic selectivities $\varphi^2_{B,1,m}/\varphi^2_{B,2,m}$*

$E = 0.1$; $\alpha = 20$; $H_{A,0} = 10^{-7.0}$; $K_A = 10^{-7.88}$; $K_R = 10^{-6.28}$.

Table 2. *Model calculations with MIRE-2: X_S as a function of $\varphi^2_{B,2,m}$ for different values of $\varphi^2_{B,1,m}/\varphi^2_{B,2,m}$*
$K_A = 10^{-7.88}$; $K_R = 10^{-6.28}$; RC: reaction-controlled.

E	α	$\frac{\varphi^2_{B,1,m}}{\varphi^2_{B,2,m}}$	$\varphi^2_{B,2,m}$	$H_{A,0}$	X_S
0.1	20	10	RC	$10^{-7.0}$	0.316
			1		0.339
			4		0.393
			10		0.462
			40		0.604
			100		0.698
			400		0.826
			1000		0.915
0.1	20	100	RC	$10^{-7.0}$	0.051
			0.4		0.072
			1		0.100
			4		0.207
			10		0.326
			40		0.525
			100		0.647
			400		0.823
			1000		0.904
0.1	20	1000	RC	$10^{-7.0}$	0.006
			0.4		0.030
			1		0.064
			4		0.182
			10		0.304
			40		0.503
			100		0.630
			400		0.810
			1000		0.892

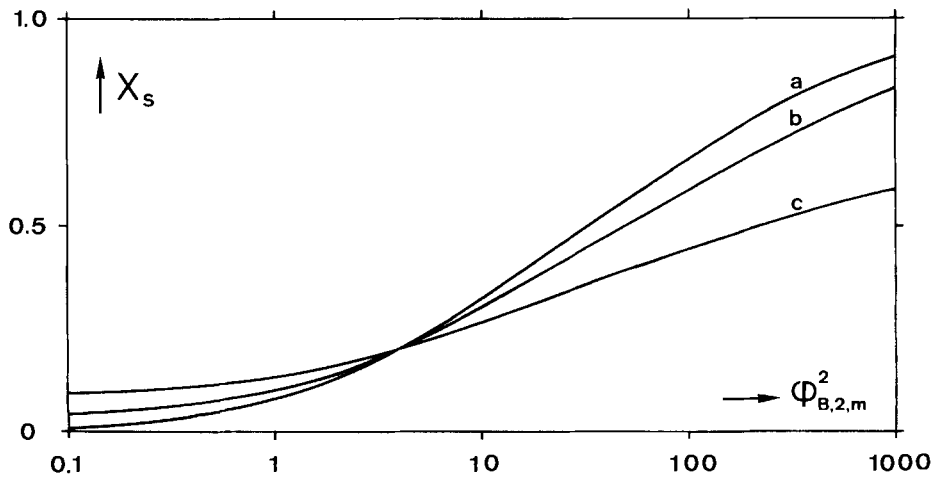

Fig. 3. *Model calculations with MIRE-PH: X_S as a function of $\varphi^2_{B,2,m}$ for different (a-c) values of $H_{A,0}$*
$E = 0.1$; $\alpha = 20$; $\Pi_{A,0} = 15$; $K_A = 10^{-7.88}$; $K_R = 10^{-6.28}$; $K_S = 10^{-6.0}$; $K_P = 10^{-8.25}$; $K_W = 10^{-12.1}$; $\varphi^2_{B,1,m}/\varphi^2_{B,2,m} = 100$; $H_{A,0} = 10^{-8.0}$ (a); $10^{-7.3}$ (b); $10^{-7.0}$ (c).

Table 3. *Model calculations with MIRE-PH: X_S as a function of $\varphi^2_{B,2,m}$ for different values of $H_{A,0}$* $K_A = 10^{-7.88}$; $K_R = 10^{-6.28}$; $K_S = 10^{-6.0}$; $K_P = 10^{-8.25}$; $K_W = 10^{-12.1}$. RC: reaction-controlled.

E	α	$\frac{\varphi^2_{B,1,m}}{\varphi^2_{B,2,m}}$	$\varphi^2_{B,2,m}$	$H_{A,0}$	$\Pi_{A,0}$	X_S
0.1	20	100	RC	$10^{-7.0}$	15	0.093
			1			0.137
			2			0.166
			10			0.269
			40			0.375
			100			0.443
			400			0.537
			1000			0.585
0.1	20	100	RC	$10^{-7.3}$	15	0.044
			1			0.101
			2			0.143
			10			0.306
			40			0.477
			100			0.587
			400			0.746
			1000			0.832
0.1	20	100	RC	$10^{-8.0}$	15	0.008
			0.4			0.036
			1			0.076
			2			0.129
			10			0.331
			40			0.530
			100			0.655
			400			0.830
			1000			0.904

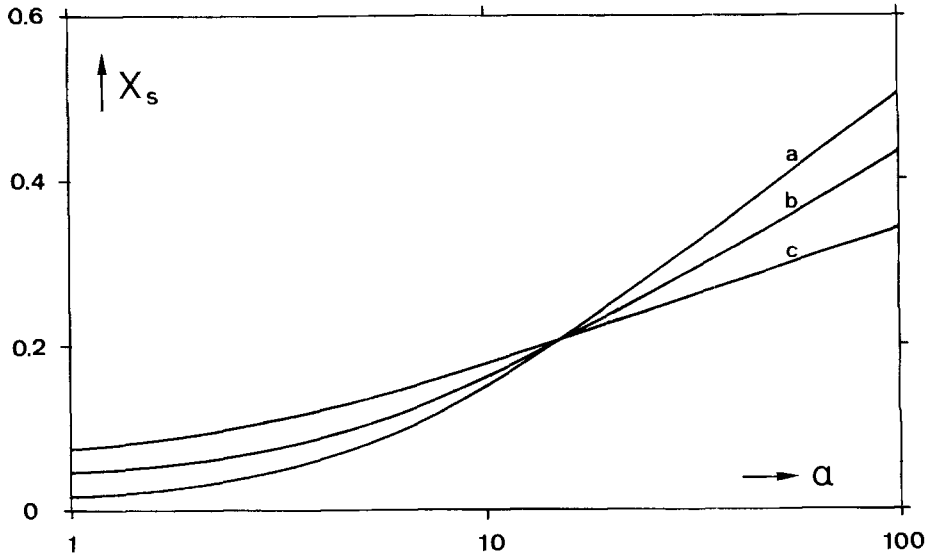

Fig. 4. *Model calculations with MIRE-PH: X_S as a function of α for different (a–c) values of $H_{A,0}$* $K_A = 10^{-7.88}$; $K_R = 10^{-6.28}$; $K_S = 10^{-6.0}$; $K_P = 10^{-8.25}$; $K_W = 10^{-12.1}$; $\Pi_{A,0} = 15$; $E \cdot \alpha = 2.0$; $E \cdot \varphi^2_{B,2,m} = 0.558$; $\varphi^2_{B,1,m}/\varphi^2_{B,2,m} = 100$; $H_{A,0} = 10^{-8.0}$ (a); $10^{-7.3}$ (b); $10^{-7.0}$ (c).

Table 4. *Model calculations with MIRE-PH: X_S as a function of* α *for different values of* $H_{A,0}$
$K_A = 10^{-7.88}$; $K_R = 10^{-6.28}$; $K_S = 10^{-6.0}$; $K_P = 10^{-8.25}$; $K_W = 10^{-12.1}$.

E	α	$\frac{\varphi^2_{B,1,m}}{\varphi^2_{B,2,m}}$	$\varphi^2_{B,2,m}$	$H_{A,0}$	$\Pi_{A,0}$	X_S
2	1	100	0.279	$10^{-7.0}$	15	0.074
1	2		0.558			0.092
0.4	5		1.395			0.134
0.2	10		2.79			0.178
0.1	20		5.58			0.228
0.04	50		13.95			0.294
0.02	100		27.9			0.344
2	1	100	0.279	$10^{-7.3}$	15	0.044
1	2		0.558			0.058
0.4	5		1.395			0.103
0.2	10		2.79			0.161
0.1	20		5.58			0.238
0.04	50		13.95			0.350
0.02	100		27.9			0.433
2	1	100	0.279	$10^{-8.0}$	15	0.016
1	2		0.558			0.030
0.4	5		1.395			0.080
0.2	10		2.79			0.151
0.1	20		5.58			0.249
0.04	50		13.95			0.395
0.02	100		27.9			0.506

Table 5. *Model calculations with MIRE-PH: X_S as a function of* $\Pi_{A,0}$ *for different values of* α
$K_A = 10^{-7.88}$; $K_R = 10^{-6.28}$; $K_S = 10^{-6.0}$; $K_P = 10^{-8.25}$; $K_W = 10^{-12.1}$.

E	α	$\frac{\varphi^2_{B,1,m}}{\varphi^2_{B,2,m}}$	$\varphi^2_{B,1,m}$	$H_{A,0}$	$\Pi_{A,0}$	X_S
1	2	100	0.558	$10^{-7.3}$	7.5	0.071
					10	0.064
					15	0.058
					30	0.054
					60	0.052
						0.050
0.4	5	100	1.395	$10^{-7.3}$	7.5	0.119
					10	0.110
					15	0.103
					30	0.097
					60	0.094
						0.092
0.2	10	100	2.79	$10^{-7.3}$	7.5	0.170
					10	0.165
					15	0.161
					30	0.158
					60	0.156
						0.155

Table 5 (continued)

E	α	$\frac{\varphi^2_{B,1,m}}{\varphi^2_{B,2,m}}$	$\varphi^2_{B,2,m}$	$H_{A,0}$	$\Pi_{A,0}$	X_S
0.1	20	100	5.58	$10^{-7.3}$	7.5	0.225
					10	0.230
					15	0.238
					30	0.246
					60	0.247
						0.248
0.04	50	100	13.95	$10^{-7.3}$	7.5	0.298
					10	0.318
					15	0.350
					30	0.382
					60	0.389
						0.392

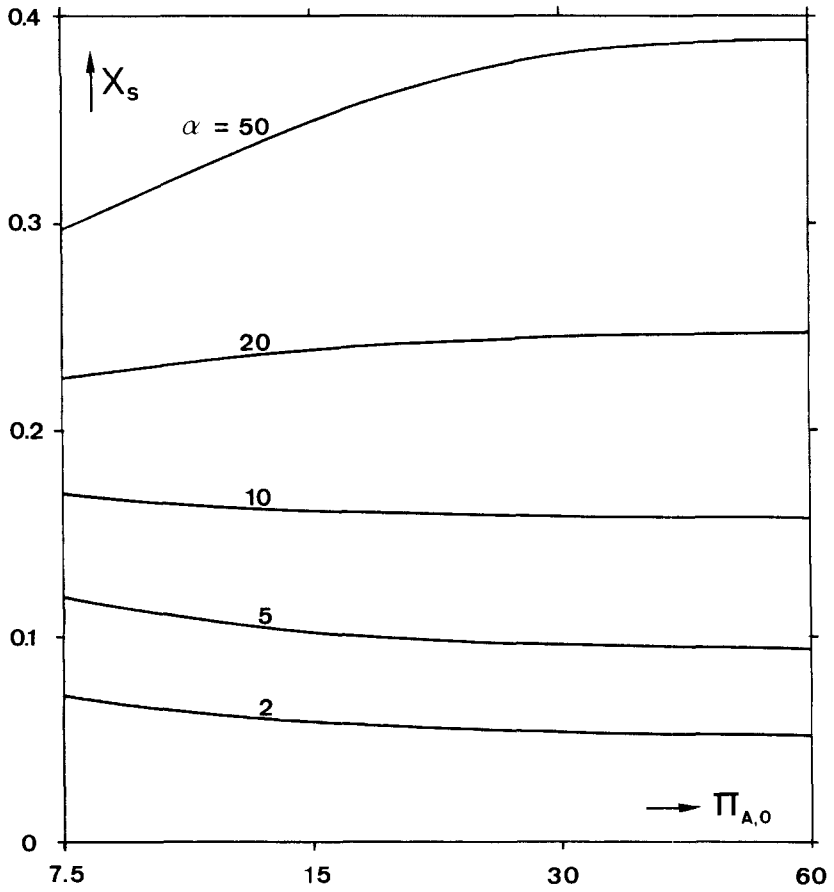

Fig. 5. *Model calculations with MIRE-PH: X_S as a function of $\Pi_{A,0}$ for different values of* α
$K_A = 10^{-7.88}$; $K_R = 10^{-6.28}$; $K_S = 10^{-6.0}$; $K_P = 10^{-8.25}$; $K_W = 10^{-12.1}$; $H_{A,0} = 10^{-7.3}$; $E \cdot \alpha = 2.0$;
$E \cdot \varphi^2_{B,2,m} = 0.558$; $\varphi^2_{B,1,m}/\varphi^2_{B,2,m} = 100$.

($\varphi^2_{B,2,m} < 1$). The behaviour is similar in *Figure 1*, where local as well as temporal changes of pH occur. However, when mixing begins to have a large influence on X_S ($\varphi^2_{B,2,m} > 10$), the product distribution continues to depend strongly on $\varphi^2_{B,1,m}/\varphi^2_{B,2,m}$ only if local pH-gradients arise *(Fig. 1)*. The reason is that the local pH change influences the pre-equilibria in such a way that the product of the concentrations of the reactive species ($AO^{\ominus}$ and $ArN_2^{\oplus}$ or $RO^{\ominus}$ and $ArN_2^{\oplus}$) decreases, the resultant slowing down of the reaction leading to a smaller mixing effect (*i.e.* a decrease in X_S) *(Fig. 1)* relative to constant pH *(Fig. 2)*. The initial pH-value determines the increase in X_S as $\varphi^2_{B,2,m}$ varies from 0.1 to 1000 *(Fig. 3)*. The initial pH loses its influence on the product distribution if it exceeds a characteristic value (here: $H_{A,0} = 10^{-8.0}$). The increase in X_S is smaller at lower initial pH-levels.

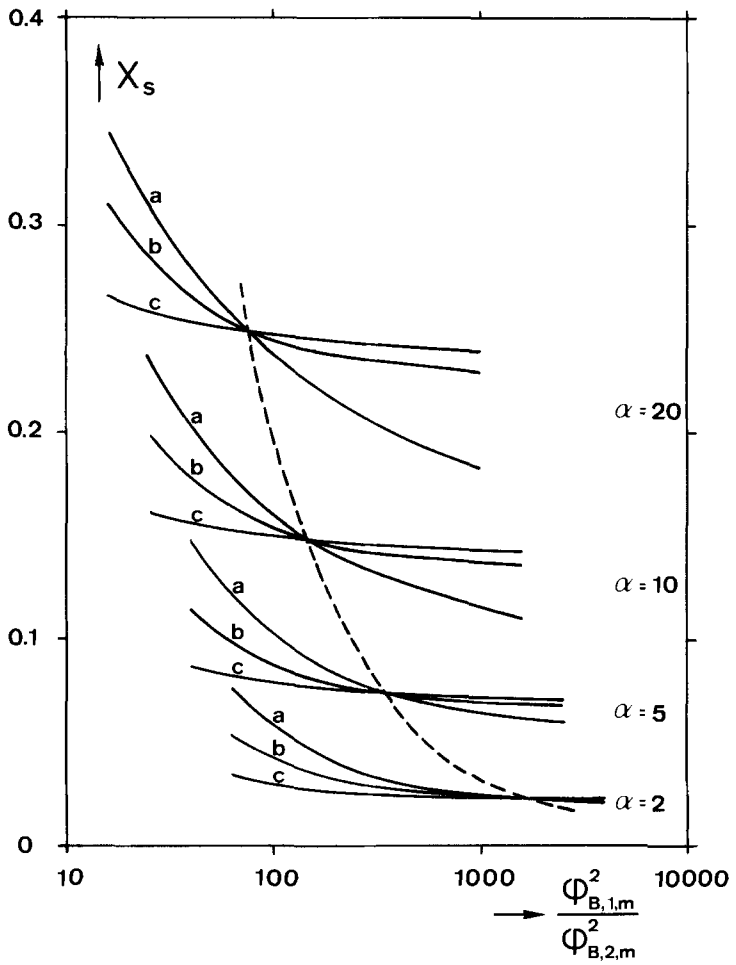

Fig. 6. *Model calculations with MIRE-PH: X_S as a function of $\varphi^2_{B,1,m}/\varphi^2_{B,2,m}$ for different (a-c) $H_{A,0}$ and α*

$K_A = 10^{-7.88}$; $K_R = 10^{-6.28}$; $K_S = 10^{-6.0}$; $K_P = 10^{-8.25}$; $K_W = 10^{-12.1}$; $\Pi_{A,0} \approx 15$; $E \cdot \alpha = 2.0$; $E \cdot \varphi^2_{B,2,m} = 0.558$; $H_{A,0} = 10^{-7.3}$ (a); $10^{-7.6}$ (b); $10^{-8.0}$ (c).

Table 6. *Model calculations with MIRE-PH: X_S as a function of $\varphi^2_{B,1,m}/\varphi^2_{B,2,m}$ for different values of $H_{A,0}$ and α*

$K_A = 10^{-7.88}$; $K_R = 10^{-6.28}$; $K_S = 10^{-6.0}$; $K_P = 10^{-8.25}$; $K_W = 10^{-12.1}$.

E	α	$\frac{\varphi^2_{B,1,m}}{\varphi^2_{B,2,m}}$	$\varphi^2_{B,2,m}$	$H_{A,0}$	$\Pi_{A,0}$	X_S
1	2	10	0.558	$10^{-7.3}$	15	0.247
		40				0.107
		100				0.058
		400				0.031
		1000				0.025
		4000				0.022
		10000				0.021
1	2	10	0.558	$10^{-7.6}$	15	0.188
		40				0.072
		100				0.043
		400				0.028
		1000				0.025
		4000				0.023
		10000				0.022
1	2	10	0.558	$10^{-8.0}$	15	0.086
		40				0.040
		100				0.030
		400				0.026
		1000				0.025
		4000				0.023
		10000				0.023
0.4	5	10	1.395	$10^{-7.3}$	15	0.299
		40				0.150
		100				0.103
		400				0.074
		1000				0.065
		4000				0.059
0.4	5	10	1.395	$10^{-7.6}$	15	0.223
		40				0.116
		100				0.089
		400				0.075
		1000				0.071
		4000				0.068
0.4	5	10	1.395	$10^{-8.0}$	15	0.127
		40				0.087
		100				0.080
		400				0.075
		1000				0.073
		4000				0.071
0.2	10	10	2.79	$10^{-7.3}$	15	0.345
		40				0.206
		100				0.161
		400				0.128
		1000				0.117
0.2	10	10	2.79	$10^{-7.6}$	15	0.271
		40				0.178
		100				0.155
		400				0.142

Table 6 (continued)

E	α	$\frac{\varphi^2_{B,1,m}}{\varphi^2_{B,2,m}}$	$\varphi^2_{B,2,m}$	$H_{A,0}$	$\Pi_{A,0}$	X_S
		1000				0.138
0.2	10	10	2.79	$10^{-8.0}$	15	0.189
		40				0.157
		100				0.150
		400				0.145
		1000				0.142
0.1	20	10	5.58	$10^{-7.3}$	15	0.405
		40				0.282
		100				0.238
		400				0.198
		1000				0.183
0.1	20	10	5.58	$10^{-7.6}$	15	0.342
		40				0.267
		100				0.247
		400				0.235
		1000				0.230
0.1	20	10	5.58	$10^{-8.0}$	15	0.278
		40				0.254
		100				0.249
		400				0.242
		1000				0.239

In *Figure 4* the stoichiometric ratio of the reactants $E\alpha$, the ratio $\varphi^2_{B,1,m}/\varphi^2_{B,2,m}$ and the magnitude $E\varphi^2_{B,2,m}$ are constant. Under these conditions, an increase in α causes an increasing disguise of the intrinsic selectivity by mixing effects. The lower the initial pH-value, the smaller this disguise by mixing.

Figure 5 shows the influence of the buffer capacity at different α-values. With increasing buffer capacity the influence of the released protons on X_S decreases. In *Figure 3* and *Figure 4* all curves intersect at a common point. At this point a change of the initial pH-value has no influence on the product distribution. Here, this point is defined as the *isoselectivity point.* The further from the isoselectivity point the experiments are carried out, the larger is the influence of the buffer capacity on the product distribution *(Fig. 5).*

Figure 6 shows the product distribution X_S as a function of the ratio $\varphi^2_{B,1,m}/\varphi^2_{B,2,m}$ at different initial pH- and α-values. $E\alpha$ and $E\varphi^2_{B,2,m}$ are taken as constant. For each curve α (resp. E and $\varphi^2_{B,2,m}$) remains constant and for each α another isoselectivity point exists. Hence, the following important point arises: The product distribution X_S characterizing the *isoselectivity points* all lie on a curve if plotted against the ratio $\varphi^2_{B,1,m}/\varphi^2_{B,2,m}$. On this curve a change in the initial pH-value has no influence on the product distribution. Here, this curve will be designated as the *isoselectivity curve.* Such an isoselectivity curve exists for each value of $E\alpha$.

In the present paper, no mathematical proof for the existence of isoselectivity points and isoselectivity curves can be given. In the next part of this series [9] some

experimental evidence for the existence of isoselectivity points will however be presented. The calculated values for the *Figures 1–6* are listed in the *Tables 1–6.*

5. Conclusion. – Mixing process can disguise the reaction rates of fast reactions and hence also the intrinsic chemical selectivity. In mixing-disguised azo coupling reactions the protons which are released during the electrophilic substitution steps cause a pH-gradient in the reaction zone. Since, owing to the acid-base pre-equilibria, these pH-gradients also determine the local concentrations of the reactants in the reaction zone, they also have an influence on the measured product distribution X_S of mixing-disguised azo coupling reactions. In addition, model calculations have disclosed the existence of characteristic sets of parameters for which the product distribution does not depend on the initial pH-value. These sets of parameters define the isoselectivity points.

Appendix

List of symbols

A	Coupling component
$AO^{\ominus}$	Naphtholate form of coupling component
AOH	Naphthol form of coupling component
$ArN_2^{\oplus}$	Free diazonium ion
$ArN_2O^{\ominus}$	Diazotate ion
ArN_2OH	Diazohydroxide
$\boldsymbol{A}_A$	Concentration of A normalized with respect to $[A]_0$
B	Diazo component
$\boldsymbol{B}_B$	Concentration of B normalized with respect to $[B]_0$
D	Diffusion coefficient $[m^2s^{-1}]$
E	Ratio of the initial concentrations of A and B; $E=[A]_0/[B]_0$
$H^{\oplus}$	Hydronium ion and higher hydrated proton
$\boldsymbol{H}_A$	Concentration of $H^{\oplus}$ normalized with respect to $[A]_0$
$\boldsymbol{H}_{A,0}$	Initial concentration of $H^{\oplus}$ normalized with respect to $[A]_0$
i	Species i
$k_{l,m}, k_{2,m}$	Intrinsic second order rate constants (rate constants for maximum rate), defined in the *Scheme* $[dm^3mol^{-1}s^{-1}]$
$k_A, k_R, k_S, k_P, k_{B,1}, k_{B,2}, k_{H_2O}, k_{-A}, k_{-R}, k_{-S}, k_{-P}, k_{-B,1}, k_{-B,2}, k_{-H_2O}$	Rate constants of n-th order, defined in the *Scheme* $[(dm^3mol^{-1})^{n-1}s^{-1}]$
K_A, K_R, K_S, K_P	Acidity constants of the species A, R, S and P $[moldm^{-3}]$
$\boldsymbol{K}_A, \boldsymbol{K}_R, \boldsymbol{K}_S, \boldsymbol{K}_P$	Acidity constants of the species A, R, S and P normalized with respect to $[A]_0$
K_W	Ionization constant of water $[mol^2dm^{-6}]$
$\boldsymbol{K}_W$	Ionization constant of water normalized with respect to $[A]_0$
P	Buffer
P^b	Basic form of buffer
P^s	Acidic form of buffer
$\boldsymbol{\Pi}_A$	Concentration of buffer normalized with respect to $[A]_0$
$\boldsymbol{\Pi}_{A,0}$	Initial concentration of buffer normalized with respect to $[A]_0$
r	Polar coordinate [m]
r_i	Specific reaction rate of species i $[moldm^{-3}s^{-1}]$
R	Monoazo product
$RO^{\ominus}$	Naphtholate form of monoazo product
ROH	Naphthol form of monoazo product
$\boldsymbol{\Omega}_A$	Concentration of R normalized with respect to $[A]_0$
$\bar{R}$	Radius of spherical eddy [m]
S	Disazo product

$SO^{\ominus}$	Naphtholate form of disazo product
SOH	Naphthol form of disazo product
Ψ_A	Concentration of S normalized with respect to $[A]_0$
t	Time [s]
T	Normalized time
V_A	Volume of surrounding solution [m^3]
V_B	Volume of eddy [m^3]
Θ	$[H^{\oplus}]_t$ normalized with respect to $[A]_0$
X_S	Measure of product distribution, defined in equ. 66
α	Ratio of eddy volume to surrounding solution volume, V_A/V_B
$\varphi^2_{B,1,m}, \varphi^{\prime 2}_{B,2,m}$	Rate constants normalized with respect to $[B]_0$ (mixing-moduli)

Special Notation

[i]	Concentration of species i [$mol\,dm^{-3}$]
$[i]_0$	Initial concentration of species i [$mol\,dm^{-3}$]
$[H^{\oplus}]_t$	Total concentration of $H^{\oplus}$, defined in equ. 21 [$mol\,dm^{-3}$]

REFERENCES

[1] *A.K. Manglik, R.B. Moodie, K. Schofield, A. Dutly, E. Dedeoglu & P. Rys,* J. Chem. Soc. Perkin II, in press (1981).

[2] *H. Belevi,* Ph. D. thesis ETH, Zurich 1980.

[3] *R.J. Ott & P. Rys,* Helv. Chim. Acta *58,* 2074 (1975).

[4] *F. Nabholz, R.J. Ott & P. Rys,* ibid. *60,* 2926 (1977).

[5] *F. Pfister, P. Rys & H. Zollinger,* Helv. Chim. Acta *58,* 2093 (1975); *F. Nabholz & P. Rys,* Helv. Chim. Acta *60,* 2937 (1977).

[6] *P. Eugster,* Ph. D. thesis ETH, Zurich 1973; *M. Aellen,* Ph. D. thesis ETH, Zurich 1977; *J.R. Bourne, P. Rys & K. Suter,* Chem. Eng. Sci. *32,* 711 (1977).

[7] *J.R. Bourne, E. Crivelli & P. Rys,* Helv. Chim. Acta *60,* 2944 (1977); *J.R. Bourne, U. Moergeli & P. Rys,* paper B3, 2nd Europ. Conf. on Mixing, Brit. Hydromech. Res. Assoc., Cranfield U.K. 1977.

[8] *A.N. Kolmogoroff,* Compt. Rend. Acad. Sci. USSR *30,* 301 (1941).

[9] *H. Belevi, J.R. Bourne & P. Rys,* Helv. Chim. Acta *64,* 1618 (1981).

[10] *M. Eigen,* Angew. Chem. *75,* 489 (1963).

[11] *G. Damköhler,* 'Einfluss von Diffusion, Strömung und Wärmetransport auf die Ausbeute bei chemisch-technischen Reaktoren', Der Chemie Ingenieur III-1. Akad. Verlagsges., Leipzig 1937.

[12] *E.W. Thiele,* Chem. Technol. *31,* 916 (1939).

[13] *S. Hatta,* Tohoku Imperial U. Techn. Repts. *10,* 119 (1932).